Adaptive Hounsfield Scale Windowing in Computed Tomography Liver Segmentation

Maciej Zakrzewski
Gdańsk University of Technology
Gdańsk, Poland *maciej.zakrzewski14@gmail.com*

Dominik Kwiatkowski
Gdańsk University of Technology
Gdańsk, Poland *domik.rex@gmail.com*

Jan Cychnerski
Gdańsk University of Technology, Faculty of Electronics, Telecommunications & Informatics,
Gdańsk, Poland *jan.cychnerski@pg.edu.pl*

Abstract

In computed tomography (CT) imaging, the Hounsfield Unit (HU) scale quantifies radiodensity, but its nonlinear nature across organs and lesions complicates machine learning analysis. This paper introduces an automated method for adaptive HU scale windowing in deep learning-based CT liver segmentation. We propose a new neural network layer that optimizes HU scale window parameters during training. Experiments on the Liver Tumor Segmentation Benchmark show that the learned window parameters often converge to a range encompassing clinically used windows but wider, suggesting that adjacent data may contain useful information for machine learning. This layer may enhance model efficiency with just 2 additional parameters.

Keywords: deep neural network layer, computed tomography, liver segmentation, hounsfield scale, liver cancer

1. Introduction and related work

Computer-assisted diagnosis (CAD) can help treat diseases such as cancer, where timely diagnosis and treatment are crucial. Liver segmentation is used in many CAD systems aiding diagnosis, surgery planning, radiation therapy, and treatment evaluation [7]. Manual tumor segmentation is time-consuming and laborious. Automating or semi-automating this process can reduce costs and improve diagnostic imaging efficiency. The Hounsfield Unit (HU) scale is used in radiological imaging to quantify the radiodensity of tissues. In Computed Tomography (CT) scans, measured HU values are often mapped to shades of grey, with different densities appearing as varying intensities on the image. Because of the wide range of HU values in CT scans, only a specific empirically derived range (window) of HU scale is viewed simultaneously to enhance the visibility of particular tissues. For example, the radiodensity of liver tissue is around 60 HU [12]. While traditionally ignored due to established human experience, out-of-range values might contain useful data for deep learning models.

Liver segmentation has been refined through various deep learning techniques, from the inception of U-net [9] to enhancements such as attention modules [5], semi-supervised learning [4], and 3D models [11]. In segmentation studies, a static pre-defined HU window is often

Work partially funded by the *Cloud Artificial Intelligence Service Engineering (CAISE)* project No. KPOD.05.10-IW.10-0005/24, KPO, European Programme IPCEI-CIS
Source code of methods and experiments is available at: `https://github.com/cvlab-ai/tomography/`

used on images to improve learning efficiency by highlighting relevant tissues. This practice is common in liver segmentation [3, 5, 6, 8, 10] and other organs like heart [13] and kidneys [2]. Window settings typically align with those used by medical professionals during CT analysis, but they can vary across studies, even for the same organ, reflecting their approximate nature [12]. Studies such as [3] and [6] have evaluated the impact of different window ranges on segmentation outcomes, showing that varying settings can significantly affect performance, with improvements around 2 percentage points in the DSC metric. These findings suggest benefits from automated methods to optimize window settings for better segmentation accuracy.

2. Proposed solution

We propose a new layer for deep neural networks called the Adaptive Hounsfield Unit Window (AHUW). This layer enhances CT image segmentation by automatically adapting the Hounsfield Unit (HU) window through learning and highlighting its range in the input data. Unlike standard HU windowing, AHUW emphasizes data within the window without discarding data outside it. AHUW can be added to any deep neural network designed for HU scale data (N-dimensional 1-channel input), placed between the input layer and the first hidden layer. During training, backpropagation updates two parameters: window width (W_W) and window level (W_L). AHUW layer transforms the complete HU range of every pixel/voxel x into a normalized interval of $[-1, 1]$, standardizing the input data and emphasizing the values within the learned HU window. The AHUW employs a two-step computational process. First, it applies a linear transformation $f(x)$, as defined in Eq. 1, where W_{min} and W_{max} are the minimum and maximum values of the HU window. The final step applies a sigmoid function $\sigma(x)$ to the transformed image, mapping the HU window to a larger interval within the output domain compared to values outside this window. The proposed neural network architecture using AHUW layer and example processed CT images are presented in Fig. 1.

$$f(x) = \frac{2\,(x - W_{min})}{W_{max} - W_{min}} - 1,\ W_{min} = W_L - \frac{W_W}{2},\ W_{max} = W_L + \frac{W_W}{2}, AHUW(x) = \sigma(f(x)) \quad (1)$$

3. Experiments

We utilized the publicly available Liver Tumor Segmentation Challenge (LiTS) dataset [1], comprising 130 CT scans from various clinics. Given the variability in tumor sizes, patients were grouped into five classes based on the percentage of tumor labels. The dataset was split into training (64%), validation (16%), and test (20%) subsets, stratified by tumor class. A patient-wise 5-fold cross-validation method was used, ensuring each patient appeared in only one fold. Scan slices lacking labels were excluded to streamline training. We evaluated the proposed solution using the Dice Similarity Coefficient (DSC) to compare baseline and modified models. DSC is a standard metric for evaluating the accuracy of spatial overlap between predicted and actual labels. The U-Net model [9], chosen for its simplicity and efficiency, served as our baseline. We used a modified binary DSC loss function, replacing the intersection operation with multiplication for smoother gradients: $loss(P, L) = 1 - 2\sum_{i,j}(P_{i,j}L_{i,j})/\sum_{i,j}(P_{i,j} + L_{i,j})$, where P is the prediction matrix, L is the label matrix. The initial learning rate was set to 10^{-5} for the U-Net model and 10^{-3} for the AHUW parameters. To improve convergence, learning rates were reduced by a factor of 0.1 after 3 epochs without a decrease in validation loss.

Experiment A. The first experiment compared the baseline U-Net model (named REF) with a modified version incorporating the AHUW layer, assessing segmentation performance and the impact of initial window settings. Results are shown in Table 1. Each row represents a different 5-fold cross-validation. The modified model was trained with 10 different starting HU windows, some corresponding to common organ windows (indicated in the Name column), across 5-fold data splits, totaling 55 training runs along with the baseline. The WW and WL columns show

the initial window width and level, respectively. Final model weights were selected based on the lowest validation loss, and DSC scores were calculated for both liver and tumor labels, averaged across 5-fold runs. Results indicate that all adaptive window models, except one (WW6000, WL2000), outperformed the reference model in average DSC. The best initial window setting (WW70, WL30) surpassed the reference model's average DSC by 0.023, a 3% improvement. On average, 70% of runs with the AHUW performed better than the baseline.

Table 1. Cross-validation DSC in Experiment A

Initial window	WW	WL	Average DSC	Std. Dev.
BRAIN	70	30	0.79494925	0.0059
SOFT TISSUE	350	50	0.79240725	0.0127
Custom 1	200	500	0.78809125	0.0103
ABDOMEN	400	40	0.78720000	0.0170
Custom 2	4000	1000	0.78702225	0.0102
LUNG	1600	-600	0.78566825	0.0090
Custom 3	400	1000	0.78458000	0.0085
BONE	2000	500	0.78252675	0.0199
LIVER	160	60	0.78050000	0.0092
REF	-	-	0.77106000	0.0166
Custom 4	6000	2000	0.76986400	0.0157

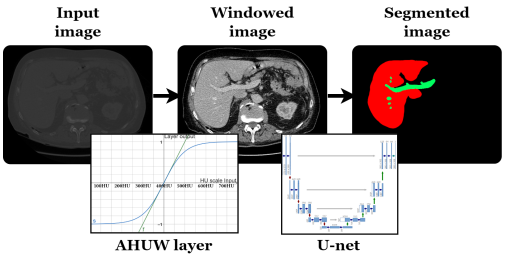

Fig. 1. Data flow in U-net with AHUW

Experiment B. Many training runs performed in Experiment A were interrupted by the early stopping procedure during initial epochs, as validation increased despite improvement in DSC. This observation suggested that the validation loss selection criterion was suboptimal. Thus, Experiment B refined the evaluation criteria. Best weight selection used the average DSC of liver and tumor classes during the validation phase instead of loss value. Moreover, besides the starting window parameters and Average DSC as previously, the average DSC for specific labels across folds and final windows parameters of AHUW layers have been recorded. 5-fold cross-validation results are summarized in Table 2. The improvement is mostly visible in DSC for the harder tumor label. The initial window setting of (WW70, WL30) was notably effective, showing a liver DSC comparable to the baseline and a tumor DSC improvement of 0.0139. The final window parameters were mostly close to common liver window settings (e.g. WW160, WL60), indicating the layer's ability to learn proper HU window parameters and aid the further segmentation process. Final windows were broader than the typical liver WW, suggesting that adjacent data typically discarded in manual segmentation might contain useful information.

Table 2. Multiclass DSC for cross-validation, and finally obtained HU windows in Experiment B

	Initial window		DSC		DSC Liver		DSC Tumor		Final Window	
Name	WW	WL	Avg.	Std. Dev.	Avg.	Std. Dev.	Avg.	Std. Dev.	WW	WL
BRAIN	70	30	0.8068	0.00664	0.9507	0.00177	0.6628	0.01203	248	62
Custom 3	400	1000	0.8054	0.00426	0.9525	0.00125	0.6582	0.00913	480	818
LUNG	1600	-600	0.8039	0.00740	0.9511	0.00381	0.6567	0.01797	890	23
SOFT TISSUE	350	50	0.8016	0.01390	0.9509	0.00236	0.6522	0.02775	361	45
LIVER	160	60	0.8006	0.00846	0.9509	0.00066	0.6502	0.01661	266	63
Custom 2	4000	1000	0.8005	0.00821	0.9503	0.00362	0.6507	0.01318	2994	686
REF	-	-	0.8000	0.00532	0.9511	0.00137	0.6489	0.00944	-	-
Custom 4	6000	2000	0.7997	0.00807	0.9522	0.00181	0.6473	0.01462	5252	1507
Custom 1	200	500	0.7939	0.02201	0.9489	0.00946	0.6389	0.03603	261	345
BONE	2000	500	0.7849	0.02962	0.9497	0.00613	0.6202	0.05345	1153	181
ABDOMEN	400	40	0.7829	0.03321	0.9455	0.01248	0.6202	0.05438	401	37

4. Summary and future work

Our research shows that integrating the proposed Adaptive HU Window Layer enhances learning efficiency with minimal computational cost. This layer, using just two parameters regardless of input size, optimizes training dynamics regardless of initial settings. Experiments confirmed that gradient optimization effectively identifies an HU window for liver segmentation, consistent with clinical standards. Models with the AHUW outperformed those without, showing improvement in 64% of results, indicating a modest yet noticeable increase in model efficacy. Future research should test the AHUW on various datasets beyond LiTS and explore its potential in multi-organ segmentation and classification tasks. Additionally, other transformations

emphasizing the HU window could further improve performance. Another promising area is to enable multiple instances of AHUW layer in the unimodal and multimodal analysis of CT images without contrast (NCCT), with contrast (CECT), and angiography (CTA), as they utilize various ranges of HU scale. Moreover, using three AHUW layers in parallel can act as a middle layer between 1-channel HU scale input and 3-channel color input for straightforward adoption of imagenet-pretrained models to CT imaging.

References

[1] Bilic, P., Christ, P., Li, H. B., Vorontsov, E., Ben-Cohen, A., Kaissis, G., Szeskin, A., Jacobs, C., Mamani, G. E. H., Chartrand, G., et al.: The Liver Tumor Segmentation Benchmark (LiTS). In: *Medical Image Analysis* 84 (2023), p. 102680.

[2] Cruz, L. B. da, Araújo, J. D. L., Ferreira, J. L., Diniz, J. O. B., Silva, A. C., Almeida, J. D. S. de, Paiva, A. C. de, and Gattass, M.: Kidney segmentation from computed tomography images using deep neural network. In: *Computers in Biology and Medicine* 123 (2020), p. 103906.

[3] Gul, S. and Khan, M. S.: On evaluating CT image enhancement techniques for deep learning based 3D liver segmentation. In: *2022 Global Conference on Wireless and Optical Technologies (GCWOT)*. IEEE. 2022, pp. 1–6.

[4] Han, K., Liu, L., Song, Y., Liu, Y., Qiu, C., Tang, Y., Teng, Q., and Liu, Z.: An effective semi-supervised approach for liver CT image segmentation. In: *IEEE Journal of Biomedical and Health Informatics* 26.8 (2022), pp. 3999–4007.

[5] Hong, L., Wang, R., Lei, T., Du, X., and Wan, Y.: Qau-Net: Quartet attention U-Net for liver and liver-tumor segmentation. In: *2021 IEEE International Conference on Multimedia and Expo (ICME)*. IEEE. 2021, pp. 1–6.

[6] Kaczor, K., Nadachowski, P., Operlejn, M., Piastowski, A., Zielonka, M., Cychnerski, J., and Kwaśniewska, A.: Comparison of image pre-processing methods in liver segmentation task. In: *2022 15th International Conference on Human System Interaction (HSI)*. IEEE. 2022, pp. 1–5.

[7] Moghbel, M., Mashohor, S., Mahmud, R., and Saripan, M. I. B.: Review of liver segmentation and computer assisted detection/diagnosis methods in computed tomography. In: *Artificial Intelligence Review* 50 (2018), pp. 497–537.

[8] Qiu, Y., Pei, Y., Li, X., Guo, S., and Li, X.: A Cascaded 3D Neural Network For Liver Tumor Segmentation. In: *2021 IEEE International Conference on Medical Imaging Physics and Engineering (ICMIPE)*. IEEE. 2021, pp. 1–7.

[9] Ronneberger, O., Fischer, P., and Brox, T.: U-net: Convolutional networks for biomedical image segmentation. In: *Medical image computing and computer-assisted intervention–MICCAI 2015: 18th international conference, Munich, Germany, October 5-9, 2015, proceedings, part III 18*. Springer. 2015, pp. 234–241.

[10] Song, L., Wang, H., and Wang, Z. J.: Bridging the gap between 2D and 3D contexts in CT volume for liver and tumor segmentation. In: *IEEE journal of biomedical and health informatics* 25.9 (2021), pp. 3450–3459.

[11] Wei, W., Rak, M., Alpers, J., and Hansen, C.: Towards fully automatic 2D US to 3D CT/MR Registration: A novel segmentation-based Strategy. In: *2020 IEEE 17th International Symposium on Biomedical Imaging (ISBI)*. IEEE. 2020, pp. 433–437.

[12] Wright, F. W.: Radiology of the chest and related conditions. In: CRC Press, 2022.

[13] Yoshida, A., Lee, Y., Yoshimura, N., Kuramoto, T., Hasegawa, A., and Kanazawa, T.: Automated heart segmentation using U-Net in pediatric cardiac CT. In: *Measurement: Sensors* 18 (2021), p. 100127.